Features in Evanescent Aharonov-Bohm interferometry.

Colin Benjamin* and A. M. Jayannavar†

Institute of Physics, Sachivalaya Marg, Bhubaneswar 751 005, Orissa, India

(Dated: February 2, 2008)

In this work we analyze an Aharonov-Bohm interferometer in the tunneling regime. In this regime, current magnification effect which arises in presence of transport currents is absent. A slight modification in the form of a quantum well incorporated in one of the arms leads to revival of current magnification. Systematics in magneto-conductance oscillations are observed in this evanescent wave geometry. In this framework we also see absence of Fano lineshapes in transmission resonances but once again one can recover these if the direct path supports propagating modes.

I. INTRODUCTION

The Aharonov-Bohm(AB) interferometer is one of the most exciting topics in mesoscopic physics research, not only because of the fundamental physical insight into questions of quantum non-locality[1] but also for being the basis of many novel phenomena at mesoscopic scales. Some of which are, persistent currents in normal metal rings[2, 3], Aharonov-Bohm oscillations[4], Fano resonances[5], and current magnification[6, 7]. In this work we analyze the local currents and conductance in this interferometer but for evanescent mode propagation. Evanescent means the incident energy of charge carrier's in the leads attached to the interferometer is less than the potential V which characterizes the ring throughout (see FIG. 1, for a schematic representation of our system). Thus when an electron with energy $E < V$ impinges on the ring it has to tunnel out of the ring. In certain situations we also consider a quantum well inserted in one of the arms of the interferometer. Only in the well and the connecting leads does the electron propagate with a real wave-vector $k = \sqrt{E}$, elsewhere it propagates with a complex wave-vector $k = i\kappa = i\sqrt{V - E}$. In such situation the contribution to conductance arises simultaneously from two non-classical effects namely, Aharonov-Bohm effect and quantum tunelling[8]. Such situation can arise when the transverse width of the ring is much less than the connecting ideal wires. In this case due to the higher zero point energy arising from transverse confinement, the fundamental sub-band minima in the ring will be at higher energy than the value of few sub-band minima in the ideal connecting wires. Now a situation can arise where propagating modes in the wire have energy less than the minimum propagating sub-band energy of the ring system. Thus the electron propagating in a lower sub-band of the ideal wire feels a barrier to it's motion (experiences an effective potential barrier V, arising solely because of the mismatch of the zero-point energies) and tunnels across the system via evanescent mode propagation. For simplicity we have restricted our calculation to single channel case. We are interested only in coherent transport, i.e., absence of dephasing. Using the wave guide method we have solved for all the scattering coefficients and wave amplitudes in the ring, required to calculate the local currents in the arms of the interferometer. For details we refer to Refs.[6, 7, 9, 10]. Expressions for
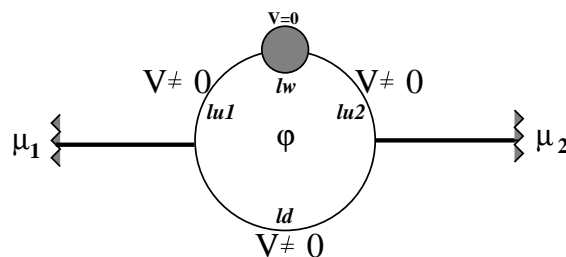

FIG. 1: The Aharonov-Bohm interferometer in the evanescent regime with a quantum well. The strength of barrier potential is V, while arm lengths are denoted in the figure.

*Electronic address: colin@iopb.res.in
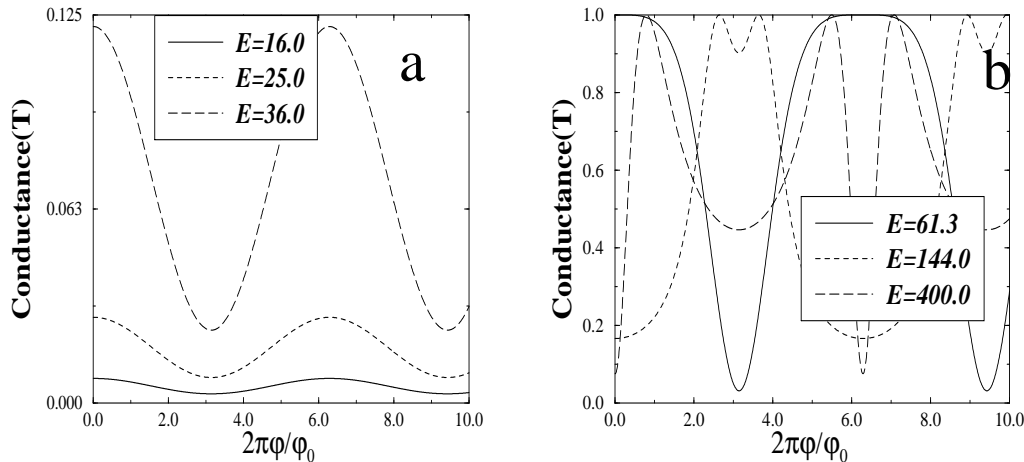†Electronic address: jayan@iopb.res.in

FIG. 2: (a) Transport in evanescent regime ($E < V$) for different Fermi energies. Systematics in magnetoconductance slopes. The lengths are- upper arm = 0.375, lower arm= 0.625, Barrier Potential = 49.0 (all in dimensional units). (b) Transport in propagating regime($E > V$) for different Fermi energies. Unsystematic nature of magnetoconductance slopes. Same physical parameters as in FIG. 2(a).

the scattering amplitudes can be obtained readily with the use of a simple MAPLE program[11]. However analytical forms of these expressions are too lengthy. Therefore we analyse our results by suitable plots generated from the obtained MAPLE expressions.

Herein we particularly analyze three configurations of the Aharonov-Bohm interferometer and see how the conductance and local currents in the two arms respond to the configurational variations. The first configuration is an AB ring at potential V attached to two leads at zero potential. In the second configuration we consider an AB ring at potential V throughout apart from the quantum well which is at zero potential, and in the final configuration we consider an AB ring with potential V only in the upper arm in addition to the quantum well but the lower arm is set free($V = 0$). In particular, we show that the first configuration does not support current magnification, while the second configuration supports it. Further the second configuration is marked by absence of Fano resonances as opposed to the third configuration. The magneto conductance shows systematic behavior as a function of flux in the evanescent regime. The detailed analysis of these phenomena is given in the following sections.

II.   EVANESCENT AHARONOV-BOHM INTERFEROMETRY

In the first configuration, we compare and contrast the cases of transport in the pure evanescent and pure propagating mode regime, with emphasis on it's conductance and local currents. In these cases the well in upper arm is absent. In FIG. 2(a), we plot the conductance in dimensionless form which is just the transmission $G = (2e^2/h)T$, as a function of the magnetic flux for different Fermi energies below the barrier potential, i.e., in the evanescent regime. The total length of the ring $l(= lu1 + lw + lu2 + ld)$ is taken to be unity and all other physical parameters of the ring are scaled with respect to this (we have set $\hbar = 2m = 1$ throughout), for example energy in dimensionless form is $El^2 \equiv E$, and barrier potential $Vl^2 \equiv V$. As expected the conductance is periodic in flux with period ϕ_0, the fundamental flux quantum $\frac{hc}{e}$. We observe that the small field differential magneto conductance is always negative. In FIG. 2(b), we plot the conductance as a function of the magnetic flux for energies above the barrier potential, i.e., in the propagating regime. We see that the small field differential magneto-conductance (MC) may be positive/negative. From these two figures we observe the systematic behavior of magneto-conductance slopes for pure evanescent wave transport in contrast to the unsystematic nature of magneto-conductance slopes for pure propagating wave transport. The systematics in transport refer to the slope of the magneto-conductance for small fields (i.e., the small field differential magneto-conductance), which for pure evanescent mode transport is always negative irrespective of the position of impurities or system parameters. Unsystematic behavior refers to this slope being very sensitive to system parameters or impurities, i.e., whether it is positive or negative cannot be predicted a priori[8].

The reason we observe the systematic nature of magneto-conductance slopes has to do with the harmonics. The harmonics are calculated as follows[12]-
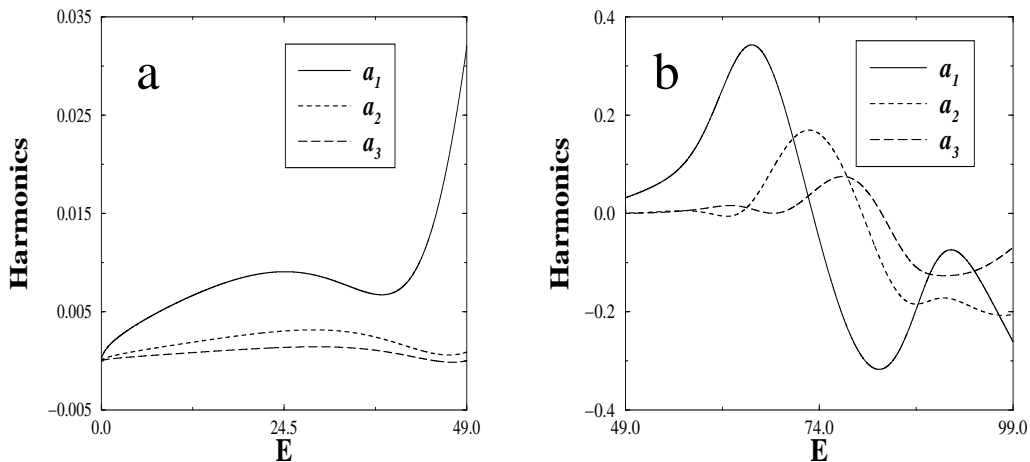
FIG. 3: (a) Complete evanescent transport. Plotted are the harmonics. Same physical parameters as in FIG. 2(a). (b) Complete propagating mode transport. Plotted are the harmonics. Same physical parameters as in FIG. 2.(a).
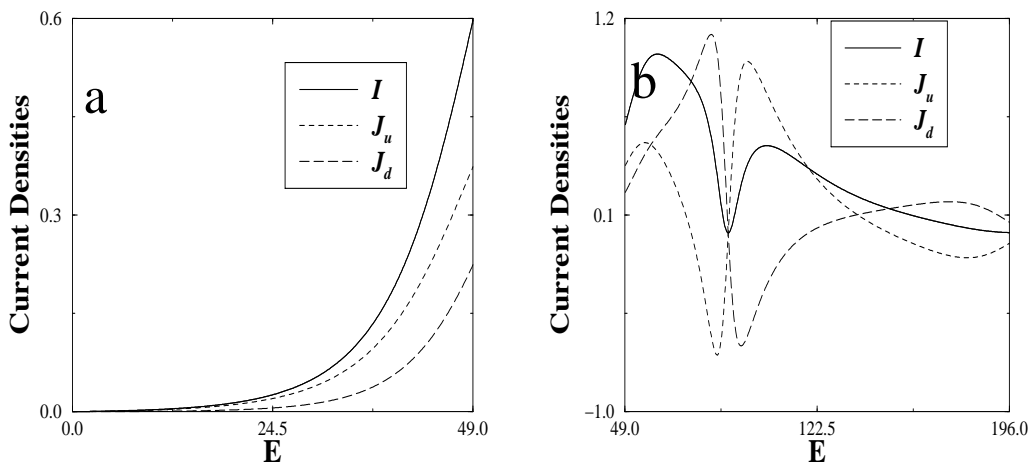

FIG. 4: (a)Current densities in the evanescent regime for zero field and increasing Energy. No current magnification. Same physical parameters as in FIG. 2(a). (b) Current densities for the propagating regime for zero field and increasing Energy. Current magnification evident. Same physical parameters as in FIG. 2.(a).

$$a_n = \frac{1}{\pi} \int_0^{2\pi} T cos(n\phi)d\phi \tag{1}$$

Herein, T represents the total transmittance and ϕ the enclosed flux. The magnitude of nth order harmonic corresponds to the contribution from electronic paths which encircle the flux n times. In the case of evanescent mode propagation the first harmonic always dominates the rest, as is seen in FIG. 3(a). Owing to the decaying nature of evanescent modes, the higher harmonics are weighted by a factor $e^{-n\kappa l}$. Thus higher harmonics, in the evanescent regime which have to encircle the ring many more times naturally decay faster(exponentially), therefore first harmonic completely dominates over the rest, and thus we see systematic behavior in the conductance and hence small field magneto-conductance slope is always negative. This definite feature (zero flux conductance is always greater than the conductance for increasing values of flux upto $\phi_0/2$, i.e., the small field regime) may be utilized in some device application which has been suggested earlier[8]. For propagating waves any harmonic can dominate over the rest (i.e., amplitude of any higher harmonic can dominate the lower one). This is amply clear from FIG. 3(b), and thus we see

unsystematic nature of slopes for small field differential magneto-conductance. In the case of propagating modes the nature of the slopes is very sensitive to system parameters and defects if present[8].

Still considering transport in the Aharonov-Bohm interferometer without the well, we plot in FIG's. 4(a) and 4(b), the output current density in dimensionless form)[6] as well as the current densities in upper J_u and lower arms J_d as a function of the incident Fermi energy for both evanescent(FIG. 4(a)) and propagating(FIG. 4(b)) modes of transport. In FIG. 4(a), we observe that the currents in the upper and lower arms are individually less than the output current, thus indicating the absence of current magnification. Now what is current magnification? In the AB interferometer, we see that the dimensionless output current density I (=T the transmission probability) around a small Fermi energy interval, flows through the system when voltage bias ($\mu_1 - \mu_2 = eV$) is applied. The upper and lower arms of the ring are of different lengths such that current densities J_u and J_d flow in these with $J_u \neq J_d$, but $I = J_u + J_d$, i.e., obeying Kirchoff's law of current conservation. In particular we see that for some particular ranges of Fermi energy J_u or J_d can be much larger than I. Current conservation thus dictates J_d or J_u to be negative[6]. This property that current in one of the arms is larger than the transport current is referred to as current magnification effect[7]. It is an effect without any classical analog in a DC circuit[7]. The negative current flowing in one arm can be interpreted as a circulating current that flows continually in the ring. The magnitude of the negative current in one of the arms flowing against the direction of applied current is taken to be that of the circulating current. When negative current flows in the upper arm the circulating current direction is taken to be anti-clockwise (or negative) and when it flows in the lower arm the circulating current direction is taken to be clockwise (or positive)[6]. It has been suggested that due to this effect one can observe large orbital magnetic moment of a ring in absence of magnetic field, however, in presence of transport currents (in non-equilibrium state). This effect has been extended to thermal currents[13] and to spin currents in the presence of Aharonov-Casher flux[14]. One can clearly see that current magnification effect is absent in the evanescent regime, as in FIG. 4(a), while being present for the propagating regime, as in FIG. 4(b). In particular from FIG. 4(b), one can see that for Fermi energy range $80.0.0 < E < 100.0$, $J_d > I$ and J_u is negative, while $J_u > I$ for $100.0 < E < 121.0$ and J_d is negative. Preferentially one observes current magnification around the anti-resonances of the ring[7]. In all the figures we have taken dimensionless parameters, the current densities J_u and J_d plotted in the figures are in their dimensionless form given by dividing J_u and J_d by $\frac{e\hbar k}{m}$.

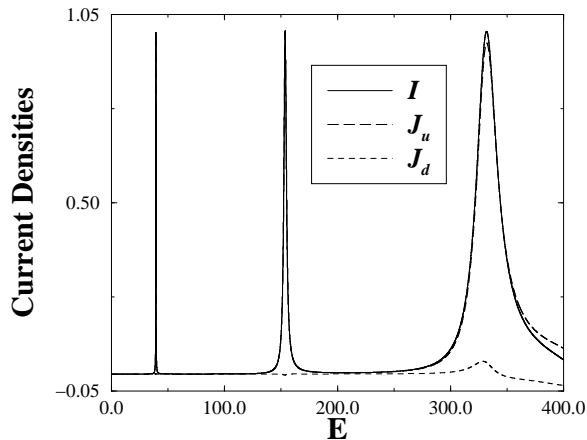## III.   EVANESCENT AB INTERFEROMETRY IN PRESENCE OF RESONANT STATES

FIG. 5: Current densities for zero field and increasing Energy. Current magnification seen at $E \leq V$. Barrier potential $V = 400.0$. Lengths are $lu1 = lu2 = 0.1$, $lw = 0.4$ and $ld = 0.4$.

Having established that evanescent mode consideration shows systematics in MC but absence of current magnification while transport in the propagating regime shows opposite behavior, no systematics in MC but current magnification is evident. Now we turn our attention to the problem as we had formulated it in our second configuration, i.e., evanescent mode transport in an Aharonov-Bohm ring with a quantum well in it's upper arm to simulate resonances. The need to incorporate resonant states arises from the fact that presence of unavoidable defects and other localized resonant states in such small devices can mar switching action and hamper device performance[8]. To analyze this if a well sustaining a few resonant states can be incorporated in the Aharonov-Bohm interferometer, then device performance can be tested. To this end we justify the inclusion of a quantum well in one of the arms. The
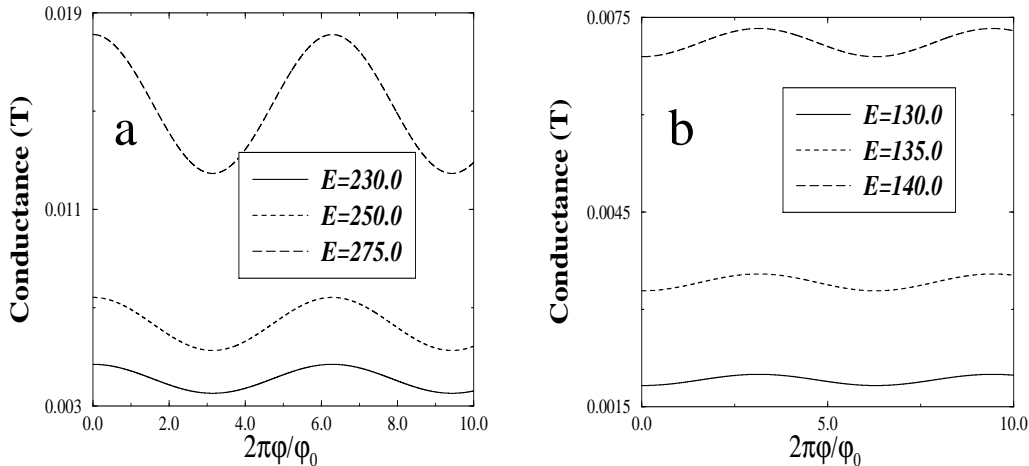
FIG. 6: Conductance for increasing field. (a) For Fermi energies to right of second resonance in FIG. 5. Same physical parameters as in FIG. 5. (b) For Fermi energies to left of second resonance in FIG. 5. Same physical parameters as in FIG. 5.

parameters defining the quantum well are mentioned in the caption of FIG. 5, in dimensionless form, l_w represents width of the quantum well, while V defines the potential barrier's, in the well region the particle is assumed to be free

In FIG. 5, we plot the output current density and the current densities in upper and lower arms as a function of the Fermi energy for asymmetric arm lengths (as in FIG. 1). We encompass three resonant states of the well. The length and height of barrier potential are mentioned in the figure caption. We assume the particle to be free in the well, i.e., in the well, potential is zero. The resonances in FIG. 5 are all of Breit-Wigner type in contrast to transmission resonances for propagating mode transport which can be either of Breit-Wigner or Fano type[7]. In contrast to evanescent transport without a quantum well, at Fermi energies comparable to barrier potential but still in the evanescent regime, current magnification is seen. The current density(J_u) of the upper arm is more than output current while that of lower arm(J_d) is negative. In this regime a circulating current continually flows in the ring even for evanescent wave transport in the region outside the well. We have also seen separately that if potential well supports many resonant states(second configuration) then also current magnification occurs at Fermi energies comparable to barrier potential and *interestingly* it is always to the right of the last resonance ($E \leq V$).

To see the effect of resonant states on the MC we plot conductance for different Fermi energies on both sides of the second resonant peak of FIG. 5, in FIG. 6(a) and FIG. 6(b). In FIG. 6(a) we plot the magneto-conductance as a function of flux for Fermi energies to right of the second resonance and left of third resonance as in FIG. 5. In FIG. 6(a) we see that the small field differential magneto-conductance is still negative and hence systematic behavior can still be seen, while in FIG. 6(b) we plot the magneto-conductance in the energy window in-between first and second resonances, and see that the small field differential magneto-conductance is positive. Thus we can draw some uniform conclusions as to where systematic action is to be seen. In particular nature of slope of magneto-conductance is always negative for Fermi energies to the left of first resonance, and then the nature of this slope (being negative or positive) alternates as we cross each successive resonance. This systematic is possible due to first, a gradual change in the transmission phase by π across the well while crossing the resonance and second due to the absence of transmission zeros in this system. The transmission zeros can lead to abrupt change in phase by π of the conductance[15, 16]. This behavior is unlike that shown in case of transport via propagating modes as seen in FIG. 2(b), where the systematics in MC cannot even be predicted due to presence of transmission zeros.

IV. QUESTION OF FANO RESONANCES

Recently Fano resonances have been observed in a mesoscopic AB ring with a quantum dot embedded in it's upper arm[5]. Fano resonances arise when a discrete set of states are coupled to the continuum[5]. Especially Fano resonances are caused by interference of two alternative paths[15], a resonant and a non-resonant one. In the geometry considered a resonant path is via a quantum well (having resonant energy levels) and a direct non-resonant path is via the lower arm of the ring (FIG. 1). Transmission resonances are generally of two types Breit-Wigner and Fano. Fano line-shapes are asymmetric as opposed to the symmetric Breit-Wigner line-shapes. In contrast to Breit-Wigner
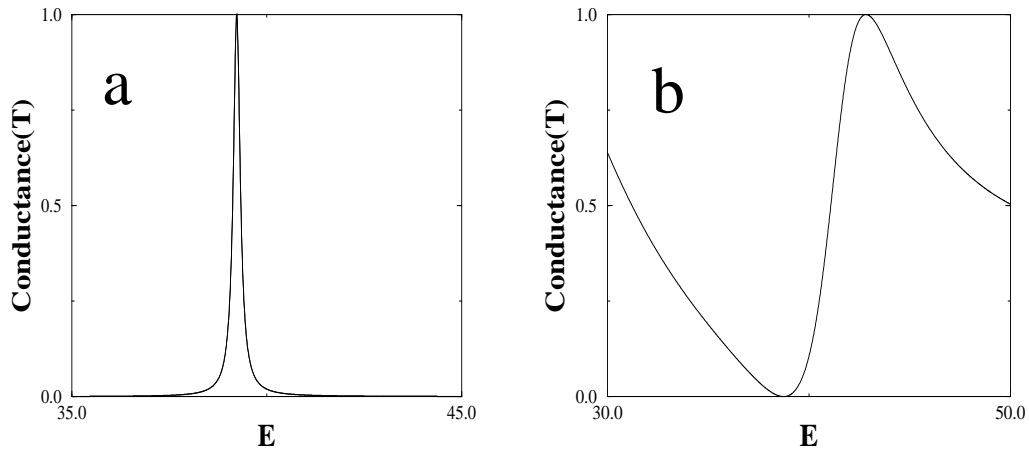
FIG. 7: (a) Evanescent transport for zero field and increasing energy. Barrier potential $V = 400.0$ and lengths are $lu1 = lu2 = 0.1, lw = 0.4$ and $ld = 0.4$, all in dimensionless units. (b) Fano resonant line-shapes. Lower arm is free (barrier absent). Same physical parameters as in (a).

forms, Fano resonances are charecterized by zero-pole pair structure in the complex energy plane of the scattering amplitude[17, 18].

In FIG. 7(a) we have plotted the conductance (in effect the transmission coefficient in dimensionless form) as function of the Fermi energy. We see resonant transport around the quasi bound states of the well (around $E = 39.0$). The line shape is that of Breit-Wigner form. We do not observe any Fano line-shapes as long as $E < V$. As mentioned earlier Fano line-shapes arise from the interference of two alternative paths, one resonant and another direct. Our results clearly indicate when the transport across the direct path is via evanescent modes, then Fano line-shapes are absent. To recover Fano line-shapes, direct path should be a propagating one. To see this explicitly we set potential in the lower arm to be zero (configuration three). So that electron traverses the lower arm as a propagating wave. For this case we have plotted in FIG. 7(b), the conductance versus Fermi energy for the same physical parameters as in FIG. 7(a). We clearly see the Fano line-shapes, i.e., line-shape is asymmetric and transmission exhibits zero around the same Fermi energy interval. The results presented in FIG.'s 7(a) and 7(b) are in the absence of magnetic field. Increasing the magnetic field which amounts to breaking the existing time reversal symmetry will lead to lifting of zeroes except when the flux piercing the loop is an integral or half integral multiple of the flux quantum[19].

V. CONCLUSIONS

To conclude, when electron traverses the entire circumference of the ring as an evanescent wave, the current magnification effect is absent. In this regime small field differential magneto-conductance is always negative. Inclusion of a well in an otherwise evanescent transport supports current magnification. The magnetoconductance shows systematic behavior even in this regime. The initial slope of the magnetoconductance alternates as we cross successive resonance peaks. The transmission resonances one observes in this set up (resonant states in an evanescent AB interferometer) are of Breit-Wigner type in contrast to the Fano line shapes expected because of the coupling between a resonant and non-resonant path. One recovers Fano resonances if transport through non-resonating path is via propagating modes. This fact emphasizes the need of a direct propagating path for observance of Fano line shapes in transmission.

[1] A. M. Steinberg, preprint cond-mat/9710046.
[2] S. Washburn and R. Webb, Rep. Prog. Phys. **55**, 1311 (1992).
[3] L. P. Levy, G. Dolan, J. Dunsmuir and H. Bouchiat, Phys. Rev. Lett. **64**, 2074 (1990); D. Mailly, C. Chapelier and A. Benoit, Phys. Rev. Lett. **70**, 2020 (1993).
[4] Y. Gefen, Y. Imry, and M. Ya. Azbel, Phys. Rev. Lett. **52**, 129 (1984).

[5] K. Kobayashi, H. Aikawa, S. Katsumoto and Y. Iye, Phys. Rev. Lett. **88**, 256806 (2002);U. Fano, Phys. Rev. **124**, 1866 (1961);A. A. Clerk, X. Waintal and P. W. Brouwer, Phys. Rev. Lett. **86**, 4636 (2001).

[6] Colin Benjamin and A. M. Jayannavar, Phys. Rev. B **64**, 233406 (2001).

[7] P. S. Deo and A. M. Jayannavar, Phys. Rev. B **50**, 11629 (1994); T. P. Pareek, P. S. Deo and A. M. Jayannavar, Phys. Rev. B **52**, 14657 (1995).

[8] P. S. Deo and A. M. Jayannavar, Mod. Phys. Lett. B **8**, 301 (1994); B. C. Gupta, P. S. Deo and A. M. Jayannavar , Int. J. Mod. Phys. B **10**, 3595 (1996).

[9] T. P. Pareek and A. M. Jayannavar, Phys. Rev. B **54**, 6376 (1996); A. M. Jayannavar and P. SinghaDeo, Phys. Rev. B **49**, 13685 (1994).

[10] J-B. Xia, Phys. Rev. B **45**, 3593 (1992).

[11] MAPLE V version 5, www.maplesoft.com.

[12] Colin Benjamin and A. M. Jayannavar, Phys. Rev. B **65**, 153309 (2002), and references therein.

[13] M. V. Moskalets, Euro. Phys. Lett. **41**, 189 (1998).

[14] T. Choi, C. M. Ryu and A. M. Jayannavar, Int. J. Mod. Phys. B **12**, 2091 (1998); T. Choi, C. M. Ryu and A. M. Jayannavar, preprint cond-mat/9808245.

[15] Ora-Entin Wohlman, A. Aharony, Y. Imry and Y. Levinson, J. of Low Temp. Phys. **10**, 3595 (2001), preprint cond-mat/0109328.

[16] P.S. Deo and A.M. Jayannavar, Mod. Phys. Lett. B **10**, 787 (1996).

[17] W. Porod, Z. Shao and C. S. Lent, Phys. Rev. B **48**, 8495 (1993).

[18] E. Tekman and P. F. Bagwell, Phys. Rev. B **48**, 2553 (1993).

[19] T. S. Kim, S. Y. Cho, C. K. Kim and C. M. Ryu, Phys. Rev. B **65**, 245307 (2002).